physica status solidi

pss

www.pss-journals.com

reprint

WILEY-VCH

Phys. Status Solidi B **252**, No. 3, 621–625 (2015) / **DOI** 10.1002/pssb.201451420

physica status solidi b
www.pss-b.com
basic solid state physics

Optical characterization of the MgO/InSe interface

T. S. Kayed[1], A. F. Qasrawi[*,2,3], and Khaled A. Elsayed[1,4]

[1] College of Engineering, University of Dammam, Saudi Arabia
[2] Department of Physics, Arab-American University, Jenin, West Bank, Palestine
[3] Group of Physics, Faculty of Engineering, Atilim University, 06836 Ankara, Turkey
[4] Physics Department, Faculty of Science, Cairo University, Giza, Egypt

Received 10 August 2014, revised 8 November 2014, accepted 13 November 2014
Published online 22 December 2014

Keywords coatings, dielectric properties, heterostructures, MgO/InSe interfaces, optical materials, terahertz devices

[*] Corresponding author: e-mail: atef.qasrawi@aauj.edu, atef.qasrawi@atilim.edu.tr, Phone: 00970599379412, Fax: 0097042510817

In this work, a 500 nm thick MgO layer deposited on the physically evaporated amorphous InSe thin film substrate is designed as a window for the MgO/InSe terahertz resonators. The optical properties including the reflectance and the dielectric constant dependence on the angle of incidence (θ_i), the normal transmittance, and the absorption coefficient of the interface were investigated in the range of ~270–1000 THz. It was observed that the total reflectivity of the substrate continuously decreases with increasing θ_i in the range of 33–80°. The spectra of InSe and MgO/InSe revealed strong dielectric resonance patterns below 450 THz. The energy bands of the direct allowed transitions in InSe film shrunk from 3.90, 2.75, and 1.49 eV to 3.71, 2.10, and 0.96 eV when MgO was deposited onto the InSe film. By analyzing the dielectric spectra, we were able to determine the static and lattice dielectric constants in addition to the oscillator and dispersion energies. The latter energy increased from 27.43 to 35.84 via interface construction.

1 Introduction InSe and MgO are very attractive materials for the fabrication of new types of optoelectronic devices in the form of thin films. Two-dimensional InSe crystal was reported to have a wealth of exotic dimensional-dependent properties [1] that makes it a promising candidate for the production of the next-generation ultra thin and flexible optoelectronic devices. Thin layers of InSe photo-conductors have been successfully prepared on rigid SiO_2/Si substrate and on flexible polyethylene terephthalate (PET) film. The relative photo responsivities of these devices were found to be 12.3 AW^{-1} at 450 nm and 3.9 AW^{-1} at 633 nm. Similarly, MgO-coated SnO_2 films prepared on plastic substrate (polyethylene naphthalate coated with indium-doped tin oxide, ITO/PEN) have been used for the production of Dye-sensitized solar cells (DSSCs) [2]. These cells reflected a maximum energy conversion efficiency of 6.5% with a high short-circuit current density of 18.1 mA cm^{-2}.

InSe and MgO thin films also play an important role in many types of electromagnetic resonance devices. Sensors made of Al/InSe/C exhibited switching properties and were found to be able to work as RF resonators [3]. The resonator exhibited a loss tangent of 10^{-7} at 3.0 GHz. Fe/MgO/Fe tunnel diodes were successfully fabricated on the top of fine-crystalline glass ceramic substrates. This device exhibited negative differential resistance and is reported to be useful in the development of magneto-resistive random access memory (MRAM) [4]. Moreover, Al/MgO/C and C/MgO/InSe/C [5] tunneling barriers are reported to be promising in producing frequency mixers and amplifiers. Thus, here in this study, we will focus on the properties of the MgO/InSe interface as a dynamic medium for electromagnetic spectrum of terahertz frequencies. Devices that operate in this frequency range are of interest nowadays due to their applicability as ultrafast photo-detectors and components in optical communication systems such as Li–Fi technology [6–8].

2 Experimental details InSe thin films were prepared by the thermal evaporation of In_2Se_3 lumps at a pressure of 10^{-6} Torr onto ultrasonically cleaned glass substrates. The thin films were then annealed at 200 °C for 1 h in nitrogen media. The scanning electron microscopy reflected better surface homogeneity of the amorphous films via heat treatment. The atomic content of the as-grown and

annealed film were found to 51.07% In and 48.93% Se and 52.4% In and 47.6% Se, respectively. The annealed film was carefully re-masked, well balanced, and painted with MgO (from Alfa Aeser). The film's thickness was measured by interferometry method and was found to be 2.1 and 2.6 μm before and after the MgO painting, respectively. The optical transmittance (T) and reflectance (R) were measured using Thermo-scientific EV300 spectrophotometer equipped with VEEMAX II variable angle reflectometer.

3 Results and discussions In order to design the MgO/InSe interface, the total reflectance of both InSe and MgO surfaces were recorded as a function of the angle of incidence (θ_i) in the range of 33–80°. The reflectivity spectra of the InSe film recoded in the frequency range of 270–1000 THz are displayed in Fig. 1. Those of MgO were previously published in another work [9]. As the figure shows, for each angle of incidence, the same spectrum is repeated but with different magnitude of total R. An interesting feature of the spectra is the emergence of interference patterns for frequencies lower than 450 THz. The most significant interference appears at 280 THz. The other two relatively strong peaks appear at 300 and 330 THz. Another interesting property of the spectra is the decrease of the amplitude of total reflectance as θ_i increases. As an illustrative example, inset 1 of Fig. 1 displays the variation of total reflectance as a function of θ_i for the strong peak that appeared around 300 THz. The R–θ_i variation is very sharp indicating the pronounced reduction of reflectance with increasing angle of incidence. Inset 2 of Fig. 1 shows that the decrease in R values is associated with slight shift in the frequency of the peak which was observed at 300 THz. The frequency linearly shifts towards higher values as the angle of incidence increases. The slope of the trend is 0.20 THz/deg.

Previous published data [9] for MgO window showed that the total reflectance increases as θ_i increases. However, that increase in R values with θ_i is not significant since the total reflectance of MgO in the studied spectral range was always less than 1%. Blocking the incident light by the top layer generally results in less light intensity reaching the absorption layer and causes severe deterioration of the photovoltaic cell performance. The effect of increase in R values of the top layer (MgO) on the absorption layer (InSe) is considerable under the Brewster angle, which is not the case for the interface here [10].

Figure 2 displays the reflectance, transmittance, and absorbance of the InSe and MgO/InSe interface in the frequency range of 270–1000 THz. It is seen that the shape of the reflectance spectrum of InSe is not altered when the MgO layer is coated. The only change appeared is the magnitude of the total reflectivity. The data displayed in Fig. 2 indicate that both of the values of R and T are decreasing with increasing incident wave frequency. The absorbance (A) was calculated from the measured R and T using the equation $A\% = 100\% - T\% - R\%$ and is illustrated in the inset of Fig. 2a. The data revealed a significant increase in the absorbance percentage when the interface is designed. The absorbance of InSe thin film at 300 THz increased from 14.6% to 44.3% after the MgO layer was deposited. Moreover, in the frequency range of 850–370 THz, the absorbance values decrease from around 65% to about 50% when the MgO layer was coated. It is worth noticing that for frequencies less than 370 THz, the absorbance increased after MgO coating. This is particularly important for the absorption of the 350 THz IR laser used in optical communication systems [11].

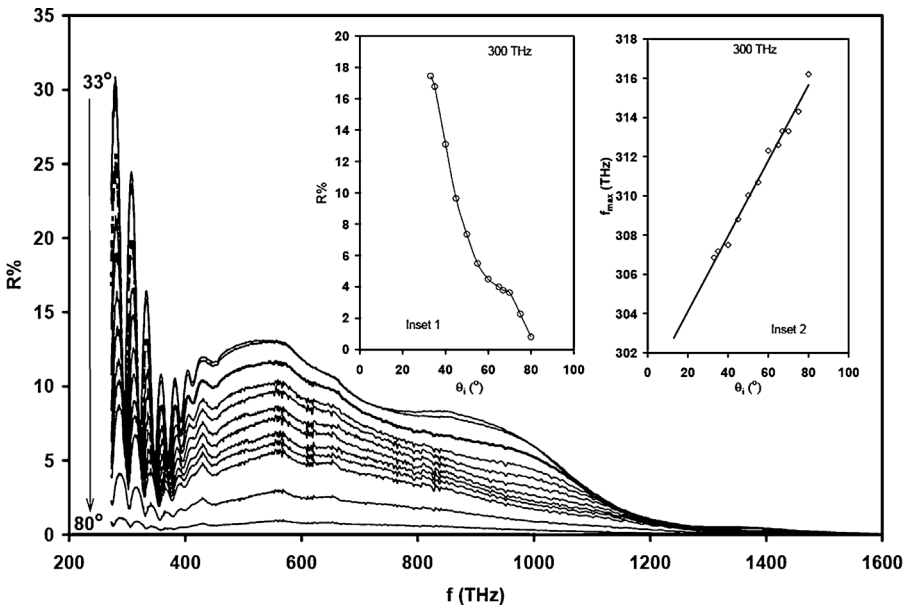

Figure 1 The incident light angle dependent reflectance of InSe thin films. Insets 1 and 2 show the R–θ_i and f_{max}–θ_i dependence at 300 THz.

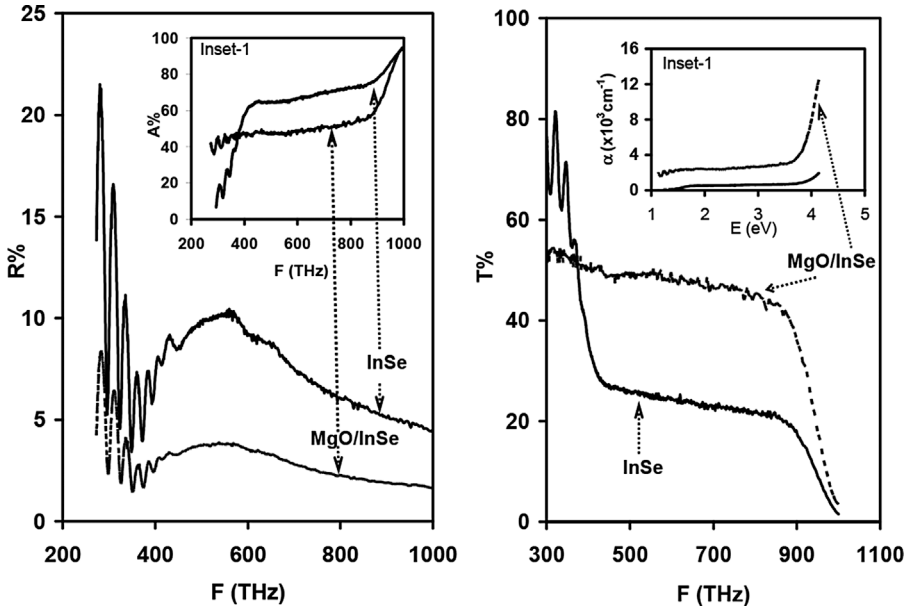

Figure 2 The frequency dependence of (a) the reflectance recorded at 45° and (b) the transmittance recorded at normal incidence. Insets: the absorbance for InSe and MgO/InSe films.

In attempting to explain the mechanism of the reflection spectra which is presented in Figs. 1 and 2, we consider the light as an electromagnetic wave. The wave which is incident on the film surface induces small oscillations of polarisation in the individual atoms, causing each atom to radiate a secondary wave in all directions. All these waves add up to give the specular reflection and refraction in accordance to the Huygens–Fresnel principle. As the MgO, InSe, and MgO/InSe films are nonconducting, the electric field of the light acts on the electrons/holes of the film surface and on the interface region during transmittance process. The moving electrons/holes generate a field and become a new radiator. The refraction of light in the film is the combination of the forward radiation of the electrons/holes and the incident light. The backward radiation is the one which is regarded as reflected from the surface of the film. In the transmission/reflection resonance peak regime, the field undergoes multiple reflections throughout the structure which result in the slowing down and confinement of light at this regime and which leads to a strong nonlinear interaction [12]. Thus, the resonance which appears at 280, 300, and 330 THz takes place whenever the incident and radiated fields couples and oscillate at the same frequency. On the other hand, whenever a phase change in the incident and radiated fields exists due to changes in the angle of incidence and/or due to the increase in the light energy, the R values are reduced and/or shifted as appeared in the insets of Fig. 1.

The T spectra of InSe films which are shown in Fig. 2b, sharply increases with decreasing frequency in the regions of 1000–870 THz and 430–357 THz. In the mid range of 860–420 THz, it slowly increases with decreasing frequency. The deposition of the MgO layer on top of InSe has changed the transmission properties of the InSe significantly. Namely, the sharp increase in T values that dominates below 430 THz has disappeared. To better understand the drastic changes in the behavior of InSe film after MgO coating, an analysis of the absorption coefficient (α) spectra is needed.

The absorption coefficient values are determined using the relation [13],

$$T = \frac{(1 - R_{\mathrm{MgO}})(1 - R_{\mathrm{InSe}})(1 - R_{\mathrm{glass}})e^{-\alpha d}}{(1 - R_{\mathrm{MgO}}R_{\mathrm{InSe}}R_{\mathrm{glass}}e^{-3\alpha d})} \quad (1)$$

with d being the film thickness and R is evaluated at normal incidence. The d values are determined from the optical reflectance using the relation

$$d = m/(2D_n\sqrt{n^2 - \sin^2\theta_i}). \quad (2)$$

Here, m is the number of fringes in wavenumber region, D_n is wavenumber region used in the calculation of thickness and n is the refractive index. The thickness of the MgO/InSe interface is determined from the related reflectance spectra and compared to those of MgO and InSe layers.

The absorption coefficient (α) spectra which are displayed in the inset of Fig. 2b are used to determine the direct allowed energy band gap (E_g) of InSe and MgO/InSe layers. It is worth mentioning that InSe thin films naturally exhibit three energy bands. The C band presented by the strong decay of α in the UV region displays a direct allowed transition type energy gap located at 3.90 eV. The A band lies in the visible region and reflects a gap of 2.75 eV. The optical energy band gap (B band) that appears in the near IR region was determined to be 1.49 eV as shown in Fig. 3. The origin of the band gap of InSe was previously investigated by A. Segura et. al. [14]. The authors reported

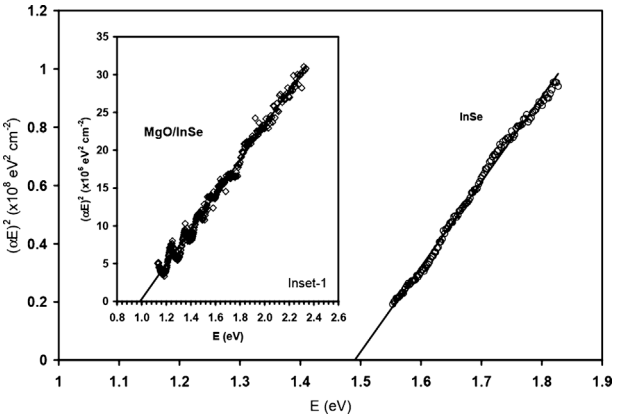

Figure 3 The $(\alpha E)^2$–E variations of InSe and MgO/InSe (Inset) thin films in the B band region.

the existence of two deeper bands with Se p_x–p_y symmetry. A valance band splitting in InSe was ascribed to the crystal field anisotropy and spin orbit interactions. The anisotropy arises from the Coulomb type attraction of Se P_x–P_y electrons with In cations being much larger than that of Se P_z electrons. While the optical E'_1 (B-band) appears to be due to the transition from the S-like to P_z-like symmetry. The other two bands known as $E_1^{/}$ (C-band) and E_1 (A-band) arise from the S-like to P_y- and P_x-like symmetries. The authors determined the value of A-band energy as 2.75 eV [14, 15] which is the same as that we have observed in this work. The C-band which was not reported by Segura et al. is calculated from the E-axis crossing of the $(\alpha E)^2$–E variation as described above.

The deposition of MgO layer over the InSe caused a shift in the value of the C, A, and B band energies from 3.90 to 3.71 eV, from 2.75 to 2.10, and from 1.49 to 0.96 eV, respectively. The respective valance band splittings are 0.19, 0.65 and 0.53 eV. The values are large enough to nominate the MgO/InSe interface as possible structure for thin film transistor production. Similar band gap offset of 0.54 eV was also detected for Cu_2O/MgO interface [16]. We have also previously shown the suitability of the MgO/InSe interface for the design of tunneling diodes through electrical characterization and the novelty of these sensors appeared from the device responsivity to microwave frequencies in the monstable-bistable modes [5]. Tamalampudi et al. [1] have also shown that InSe photodetectors fabricated on both a rigid SiO_2/Si substrate and a flexible polyethylene terephthalate (PET) film, are sensitive to broadband photodetection in the region of 450–785 nm with high photoresponsivities up to 12.3 AW^{-1} at 450 nm (on SiO_2/Si) and 3.9 AW^{-1} at 633 nm (on PET).

The decrease in the E_g of InSe upon heterojunction construction may be attributed to the difference in electron affinities of MgO (0.85 eV) and of InSe (4.55 eV) films [5]. It can also be attributed to the difference in the valance and conduction band offsets of MgO and InSe in addition to the dipole layer at the interface between MgO and InSe [17]. The dipole layer arises from the electron tunneling from the conduction band of one material into the E_g of the other material [5, 17].

To extend the applications possibilities of this structure we now turn the attention to the dielectric properties of the MgO/InSe heterojunction. The effective dielectric constant (ε_{eff}) of the MgO/InSe interface is calculated from the reflectance data for a beam of light perpendicularly polarized to the plane of incidence (R_S) using Fresnel's equation [19].

The measured R that is presented in Fig. 1 represents the total reflectivity of both parallel (R_p) and perpendicular (R_s) light wave polarizations with $R = (R_p + R_s)/2$. At an angle of incidence of 45° there is $R_p = R_s^2$, thus ε_{eff} can be directly evaluated from Fresnel equations for either R_s or R_p.

The real (ε_r) and imaginary (ε_i) components of the effective dielectric constant ($\varepsilon_{eff} = \varepsilon_r + i\varepsilon_i$) are displayed in Fig. 4 and its first inset. In general, the dielectric constant of the MgO/InSe interface which is evaluated in the frequency range of 270–1000 THz exhibit a smooth increase followed by invariant and then sharply falling trends in the frequency ranges of 1000–544, 545–494, and 495–437 THz, respectively. In the range of 436–270 THz, the effective and real dielectric spectra display few resonance peaks that increase in amplitude with decreasing frequency. The three well pronounced peaks that appear at resonance frequencies of 337, 310, and 283 THz exhibit a resonance full width at half maximum (FWHM) of 13.0, 14.8, and 13.7 THz, respectively. The values of ε_i are very low compared to those of ε_r. This indicates low tangent loss and high quality factor (Q). The Q factor spectra displayed in the second inset of Fig. 4 are generally greater than 100, which is the acceptable value for well performing devices.

The values of the FWHM are important parameters as they indicate the duration of pulse waveforms and the spectral width of sources used for optical communications. This bandwidth means that the width of frequency range where less than half the incident light power is attenuated is ~14 THz. In other words, the incident light power is at least half the maximum Thus, for intense light pulses in the 270–

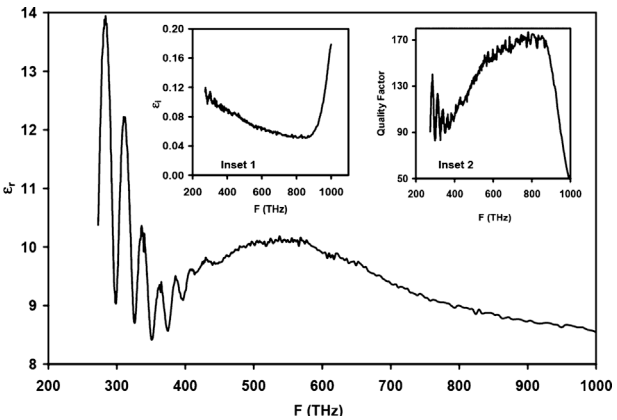

Figure 4 The frequency dependence of ε_r for MgO/InSe heterojunction. Inset-1 and inset-2 display the ε_i and the quality factor, respectively.

450 THz terahertz spectral range, a stable electromagnetic waveform could serve as adjustable bias [18].

Variations of $(\varepsilon_{eff}-1)^{-1}$–$E^2$ and ε_{eff}–λ^2 for the MgO/InSe interface were plotted (not shown) according to the single oscillator model [19] in the frequency range of 500–440 THz. This frequency range is the most allowed dispersive region. From the plots, the dispersion energy (E_d), the oscillator energy (E_o), the static dielectric constant (ε_s), and the lattice dielectric (ε_l) constants were determined to be 35.84, 4.81, 8.45, and 11.50, respectively. The same parameters were calculated for the InSe substrate and found to be 27.43, 3.19, 9.60, and 20.66, respectively.

The difference between ε_s and ε_l for InSe and MgO/InSe interface may be assigned to the free charge carrier contribution [20]. The total contribution to the dielectric constant is shared by the free space (ε_o), lattice contribution, and electronic contribution. The latter is composed of the free carriers and the entire set of valence electrons [20]. Changing the frequency of the incident wave alters the response of the electrons and of the lattice to the time dependent light spectrum. In the absence of free carriers, the dielectric constant is static. This explains the reason beyond the variation in ε_s (9.60 for InSe and 8.45 for MgO/InSe) and the strong variation in ε_l from 20.66 to 11.50 when InSe is interfaced with MgO. As the MgO layer contributes holes to the InSe layer (n-type) layer, the lattice vibration is reduced. In contrast, since the electronic contribution of the MgO to the InSe film is poor, the changes in the values of ε_s are less apparent.

4 Conclusions A new evaluation for the MgO/InSe interface is presented by optical characterization of this heterostructure in the incident wavelength range of 300–1100 nm. The dependence of the reflectance and dielectric spectra of light is studied. In addition, the absorption and dielectric spectra are analyzed to establish the optimum parameters of the interface. It was shown that the resonance peaks that appeared at the terahertz frequencies are less affected by the MgO window. The window increased the oscillator energy of InSe from 3.19 to 4.81 eV. It also reduces two of the energy bands of InSe by greater than 0.5 eV which is the value needed for the design of thin film transistors.

Acknowledgements This work was funded by the Deanship of Scientific Research at the University of Dammam under project number 2014139.

References

[1] S. R. Tamalampudi, Y. Y. Lu, R. U. Kumar, R. Sankar, Ch.-Da Liao, K. B. Moorthy, Ch. H. Cheng, F. Ch. Chou, and Y. T. Chen, Nano Lett. **14**, 2800 (2014).
[2] Sh. Li, Z. Chen, Y. Wang, T. Li, B. Xu, and W. Zhang, J. Electrochem. Soc. **161**, H6 (2014).
[3] A. F. Qasrawi, Phys. Scr. **89**, 065802 (2014).
[4] A. Filatov, A. Pogorelov, and Y. Pogoryelov, Phys. Status Solidi B **251**, 172 (2014).
[5] A. F. Qasrawi, Mater. Sci. Eng. B **178**, 851 (2013).
[6] L. Li, L. Chen, J. Zhu, J. Freeman, P. Dean, A. Valavanis, A. G. Davies, and E. H. Linfield, Electron. Lett. **50**, 309 (2014).
[7] K. I. Zaytsev, I. N. Fokina, A. K. Fedorov, and S. O. Yurchenko, J. Phys. Conf. Ser. **486**, 012024 (2014).
[8] P. Daukantas, Opt. Photon. News **25**, 34 (2014).
[9] A. F. Qasrawi, M. M. Abd-Alrazq, and N. M. Gasanly, J. Alloys Compd. **583**, 180 (2014).
[10] L. Zhua, J. K. Luoa, G. Shao, and W. I. Milne, Sol. Energy Mater. Sol. Cells **111**, 141 (2013).
[11] D. Burghoff, T. Y. Kao, N. Han, Ch. W. I. Chan, X. Cai, Y. Yang, D. J. Hayton, J. R. Gao, J. L. Reno, and Q. Hu, Nature Photon. **8**, 462 (2014).
[12] J. Lekner, Theory of Reflection of Electromagnetic and Particle Waves (Springer, Hingham, 1987).
[13] J. I. Pankove, Optical processes in semiconductors (Prentice-Hall, New Jersey, 1971), p. 94.
[14] A. Segura, J. Bouvier, M. V. Andrés, F. J. Manjon, and V. Munoz, Phys. Rev. B **56**, 4075 (1997).
[15] N. Kuroda, I. Munakata, and Y. Nishina, Solid State Commun. **33**, 687 (1980).
[16] X. Wang, D. Yan, Ch. Shen, Y. Wang, W. Wu, W. Li, Zh. Jiang, H. Lei, M. Zhou, and Y. Tang, Opt. Mater. Express **3**, 1974 (2013).
[17] S. Adach, Properties of Aluminum Gallium Arsenide, EMIS data reviews series, no. 7 (IEE, INSPEC, London, 1993).
[18] O. Schubert, M. Hohenleutner, F. Langer, B. Urbanek, C. Lange, U. Huttner, D. Golde, T. Meier, M. Kira, S. W. Koch, and R. Huber, Nature Photon. **8**, 119 (2014).
[19] M. Fox, Optical Properties of Solids (Oxford University Press, New York, 2001).
[20] D. Ferry, Semiconductor Transport (Taylor & Francis, London, 2000).